http://ansinet.com/itj

ITJ

ISSN 1812-5638

INFORMATION TECHNOLOGY JOURNAL

ANSInet
Asian Network for Scientific Information
308 Lasani Town, Sargodha Road, Faisalabad - Pakistan

Information Technology Journal 12 (1): 97-104, 2013
ISSN 1812-5638 / DOI: 10.3923/itj.2013.97.104

3D Image Reconstruction for Implosion Pellet in ICF Experiment Based on Iterative Algorithms

[1]Jianping Xia, [2]Shaorong Chen, [3]Songhua He, [2]Xishun Liu and [4]Hanzhong Guo
[1]School of Information Science and Engineering, Hunan University, 410082 Changsha, China
[2]College of Electronic Science and Engineering, National University of Defense Technology, 410073 Changsha, China
[3]School of Information Science and Engineering, Hunan University, 410073 Changsha, China
[4]School of Information Science and Engineering, Hunan University, 410012 Changsha, China

Abstract: The projection images of implosion-pellet captured by framing cameras or pinhole cameras are two-dimensional in the inertia confinement fusion experiments. Since the two-dimensional images are lack of the depth information, therefore they are hardly used to diagnose the compression symmetry of the implosion-pellet, the 3D image of the implosion-pellet reconstructed from their two-dimensional projection images can overcome these problems. As the iterative algorithms can reconstruct the original 3D image from just a few projections with good noise suppression, three iterative algorithms which are commonly applied in CT image reconstruction filed are utilized to the reconstruct 3D image of implosion-pellet. The numerical simulations show that the algebraic reconstruction technique algorithm performs best under the condition that the projection images are 'incomplete' and noise free or with not so heavy noise. When there are heavy noise in the projection images the simultaneous iterative reconstruction technique surpasses the other algorithms, which is proved to be more competent for the 3D image reconstruction of implosion-pellet in inertia confinement fusion experiment.

Key words: Inertia confinement fusion, algebraic reconstruction technique, simultaneous iterative reconstruction technique, simultaneous algebraic reconstruction technique, three-dimensional reconstruction

INTRODUCTION

The basic idea of Inertia Confinement Fusion (ICF) is to use a laser or X-ray to evenly irradiate the shell of micro-spherical pellet, which is filled with deuterium and tritium fuel, to form plasma layer with high temperature and pressure. As the plasma expands, the pressure created makes the pellet compressed inwardly to compress the deuterium and tritium fuel layer to reach a density as high as hundreds of grams per cubic centimeter of the quality. Therefore, it can force partial deuterium and tritium areas to generate high temperature and high density hot spots in order to reach the ignition conditions (He, 2000; Peng *et al*., 2011). Two laser ICF pellet drive methods exist in the literature, i.e., direct drive and indirect drive. The former is to let laser energy directly and uniformly irradiate pellet shell to obtain symmetry and high gains of implosion. While the latter is to put the pellet in the sheath cavity and then make the laser energy irradiate the inner wall. The wall absorbs the energy to generate X-ray, which then irradiates pellet and thus leads to nuclear fusion (Zhang and Chang, 2004). Both methods, however, require an even irradiation on the pellet in order to compress the pellet symmetrically. To achieve efficient pellet implosion, quantitative measure of the uniformity of laser or X-ray irradiation and the symmetry of pellet compression is needed. Traditional framing cameras or pinhole cameras capture two-dimensional projection images of the three-dimensional spherical implosion pellet. It records the contours of the pellet without more details. But, they can not record the pellet compression density changes during the process of experiment and therefore are difficult to achieve a higher diagnostic accuracy (Yuan *et al*., 2009). 3D diagnostic techniques can produce the three-dimensional images, which makes the uneven position of the pellet be accurately located and degree of nonuniform distribution quantitatively measured.

The ICF experiment usually takes a few time (in the order of ns) and the observable angles are limited.

Corresponding Author: Jianping Xia, ATR Laboratory, National University of Defense Technology, Changsha, 410073, Human, People's Republic of China

Besides, there can not be a lot of cameras to monitor ICF experiment, for the consideration of their high cost. Therefore, the projection data obtained in ICF experiments always is 'incomplete'. For the reconstruction of using 'incomplete data', iterative methods which are based on estimation theory are believed to perform better results than the transformation-based methods (Zhuang, 1992; Anders, 1989). An initial intensity is firstly provided to each pixel in the reconstruction area and the iteration begins which updates the pixels' intensity according to some a criterion and stops when the acceptable image is obtained (Zhang, 2008). The iterative methods mainly include Algebra Reconstruction Technique (ART), Multiplicative Algebraic Reconstruction Technique (MART), Simultaneous Algebraic Reconstruction Technique (SART), Simultaneous Iterative Reconstruction Technique (SIRT). The iterative algorithms can archive high spatial and density resolution of the reconstructed images and the high quality reconstruction even using incomplete projection data (Bin *et al*., 2008; Buzmakov *et al*., 2011).

The whole work is organized as follows: three classical algorithms in CT image reconstruction filed are introduced firstly. Then, the three-dimensional numerical model of the pellet is constructed according to ICF experiment. Iterative algorithms are utilized to reconstruct that model to simulate the reconstruction process of density distribution from the projection data obtained from ICF experiment. Since the data can only be obtained from a limited number of cameras and is always contaminated by noise, four projection directions are adopted in our simulation experiment and the reconstruction accuracy of the three algorithms are compared with respect to different noise levels. The numerical simulation results show that the ART algorithm performs best in the projection data without noise, while the SIRT algorithm archives best constructed image when projection data contaminated by a certain intensity Gaussian noise (such as 15 dB).

THE INTRODUCTION OF ITERATIVE ALGORITHMS

Algorithms models: Iterative reconstruction algorithms discretize the continuous image f(x, y) and imaginary square grids are superimposed over the plane on which the image is to be reconstructed, as shown in Fig. 1. The width of each grid is σ. Assume that the pixel intensity in each grid is uniform but different from other pixels. The image is expressed as an one-dimensional array $f = [f_1, f_2, \ldots, f_N]$, $N = n\times n$. Where f_j denotes the pixel intensity of jth grid. $p = [p_1, p_2, p_2, \ldots, p_M]$ is an

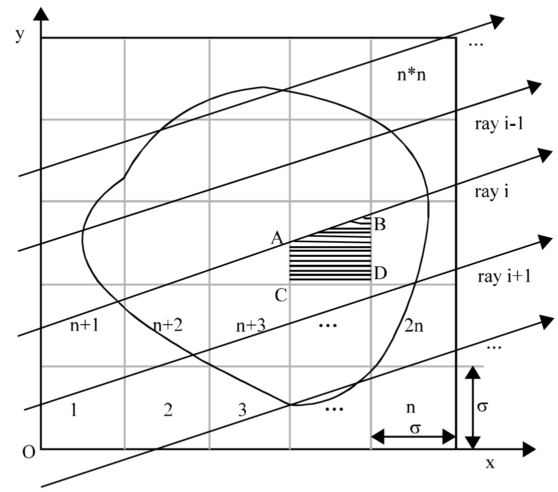

Fig. 1: Projection schematic

one-dimensional vector consisting of M ray projection data. Where M is the total number of X-rays, i.e., it is the product of projection numbers and the ray numbers in each projection direction.

$W = \{w_{ij}\}_{M\times N}$ is the coefficient matrix with M rows and N columns and w_{ij} is the weigh which represents the contribution of Jth pixel to the ith ray projection sum. The calculation of projection coefficients is determined by the model selected (Zhang, 2005). In all the three models, ray beams are assumed to be parallel with different width and interval and weigh expressions.

Model 1: The rays are modeled as parallel ray beam, whose width is σ and interval is 0. Therefore, the ray covers partial area of the grid and w_{ij} is calculated as the ratio of surface covered by ith ray in the jth pixel grid:

$$w_{ij} = \frac{S_{ABCD}}{\sigma^2} \quad (1)$$

Model 2: The width of parallel ray beam is σ and its interval is 0, but w_{ij} indicates whether the ray i pass through the pixel j or not. It can be expressed as:

$$w_{ij} = \begin{cases} 1 & \text{Ray i pass the center of pixel k} \\ 0 & \text{The others} \end{cases} \quad (2)$$

Model 3: The rays are assumed to be parallel with width 0 and the interval σ. W_{ij} represents the length of the grid j and the ray i intersects the line segment l_{AB}.

The quality of reconstructed image is best under model 1 but the calculation of projection coefficients is very complex and time-consuming, so it ultimately slows the convergence of iteration. In order to accelerate the iteration, the projection coefficient is simplified to 1 or 0 in model 2. But this kind of simplification introduces more errors, which makes the reconstructed image always contain 'salt and pepper noises' (Herman, 1980). The iteration in model 3 converges faster than that in model 1 and the constructed image is as good as that by model 1. Therefore, the model 3 will be adopted to calculate the projection coefficients w_{ij}.

Algebra reconstruction technique (ART): ART (Guo and Chen, 2009; Zhang *et al*., 2007) algorithm was firstly proposed by Herman (1980) for the reconstruction of discretization digital images. From the view of mathematics, ART actually utilizes the iterative method introduced by Kaczmarz (1937) to solve the large linear systems with a sparse coefficient matrix.

ART can be depicted by solving the following equations:

$$\sum_{j=1}^{N} w_{ij} f_j = p_i \qquad i = 1, 2, \ldots, M \tag{3}$$

Equation 3 can be rewritten as WF = P in matrix form. The analytic method is very difficult to solve such equation for that the matrix W is a large sparse matrix and thus its inverse matrix is hardly to find out. Therefore, the relaxation iterative method is always used to resolve such problem.

The initial value of F in iterations is $F = F^0$ and vector F^0 is usually set to zero. And the iteration runs as following equation:

$$F^{k+1} = F^k + \lambda^k \frac{p_{i_k} - w_{i_k}^T F^k}{\left\| w_{i_k} \right\|^2} w_{i_k} \tag{4}$$

where, i_k = [k(mod)M+1], λ is the relaxation parameter ($0 \le \lambda \le 2$), which can be used to accelerate the iteration and eliminate the noise. k is the iterative steps, w_{ij} is the i_k row of the coefficient matrix. A single iteration of the above formula means that a back projection operation is done for a ray, which means these intensities of the pixels passed through by that ray will be updated. This iteration stops until all the convergence conditions are satisfied.

Simultaneous iterative reconstruction technique (SIRT): The SIRT (Liu, 2004; Liang-Zhong *et al*., 2007) algorithm which is similar to ART is also an iterative reconstruction algorithm. It is designed to make the reconstruction process more robust to measurement noise. For ART algorithm, only one ray's projection is used in each iteration. In this case, the solution will also be influenced if the measured value of the projection of this ray contains errors. The least squares criterion can be used to reduce the error. Equation 3 can be rewritten as follows by adding an error matrix E:

$$P = WF + E \tag{5}$$

And the optimum matrix F can be obtained by minimum $\varphi(F)$ expressed as follows:

$$\varphi(F) = (P - WF)^T (P - WF) \tag{6}$$

So the optimum matrix F should satisfy the following equation:

$$W^T P = W^T W F \tag{7}$$

where, P is the vector of projection measurements and W^TP is the back projection of P. WF represents the pseudo ray sum and W^TWF is the back projection of WF. Equation 7 means that the back projection reconstruction result of the measured projection vector should be the same with the reconstruction result of the pseudo ray sum. That is the back projection value of the ray sum gained by estimating the image equals to the back projection value of the measured projection.

The whole iteration of SIRT algorithm can be expressed in following equations:

$$F^0 = W^T P \tag{8}$$

$$\begin{aligned} F^{(k+1)} &= F^{(k)} + \lambda^{(k)} (W^T P - W^T W F^{(k)}) \\ &= F^{(k)} + \lambda^{(k)} W^T (P - W F^{(k)}) \end{aligned} \tag{9}$$

Equation 8 means that the back projection of the measured projection data is set as the initial value of the image to be reconstructed. The estimated image vector $F^{(k)}$ of kth iteration adds the correction items to get the image vector $F^{(k+1)}$ and the correction items are proportional to the estimated error vector (W^TP-$W^TWF^{(k)}$) of the kth iteration. Therefore, the correction items of every pixel intensity is the error accumulation of the ray sum of the rays passing through this pixel, instead of only one ray, which is the fundamental difference between SIRT algorithm and the ART algorithm. And that is also the key reason that SIRT is able to effectively inhibit the noise contained in the measurement projection data. The correction process of SIRT is known as the 'point after point correction' relative to the 'line after line correction' of the ART algorithm.

Simultaneous algebraic reconstruction technique (SART): SART, proposed by Andersen and Kak (1984), is an algebraic reconstruction method. The difference between this algorithm and the two algorithms described above is that the correction item of each pixel is the error accumulation of ray sum of that rays through this pixel in the same projection angle, which is actually used to smooth the noise in ART. SART algorithm combines the advantages of the SIRT algorithm for high-quality reconstruction, while avoiding the shortcomings of large memory capacity and slow convergence. The iterative equation is as follows:

$$f_j^{(k+1)} = f_j^{(k)} + \frac{1}{\sum_{p_i \in p_\varphi} w_{ij}} \sum_{p_i \in p_\varphi} [\lambda \frac{p_i - \sum_{n=1}^{N} w_{in} f_n^{(k)}}{\sum_{n=1}^{N} w_{in}}] w_{ij} \quad (10)$$

where, p_φ denotes the measured projection value of all the rays in the projection orientation φ.

COMPUTER NUMERICAL SIMULATION AND RESULTS ANALYSIS

Generally, 3D data reconstruction can be classified into two categories. The first one reconstructs the two-dimensional tomography image from the projection data and then constitutes the three-dimensional images from two-dimensional image. The other one reconstructs three-dimensional image directly from two-dimensional projection data. The former fits best for the reconstruction from the parallel beam projection, while the latter is best suitable for the cone-beam projection. In present study, the first method is adopted to convict 3D reconstruction according to the ICF experiment context.

The choice of reconstruction model, projection direction and error indicators: In the numerical simulation, the reconstruction area will be divided into 60×60×60 voxels. The reconstruction model consists of two balls with different density, nested within each other. There are a big ball and a small ball with the radius of 25 and 9 with the density of 8 and 3, respectively. The sphere center distance of the two balls can be expressed as $O_1O_2 = 3$, which is shown in Fig. 2. A mathematical equation is:

$$I(x,y,z) = \begin{cases} 8 & (x-3)^2 + y^2 + z^2 < 9^2 \\ 3 & x^2 + y^2 + z^2 < 25^2 \\ 0 & \text{others} \end{cases} \quad (11)$$

Projection calculated using the coordinate system is shown in Fig. 3, if plasma X-ray self-absorption is not considered, the projection data obtained by the line integral along the projection direction r, as follows:

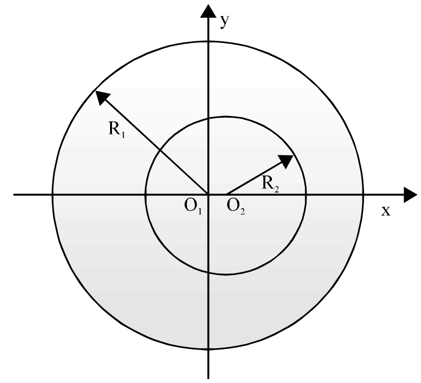

Fig. 2: Reconstruction model (Z = 0 section), R_1: The radius of O_1, R_2: The radius of O_2

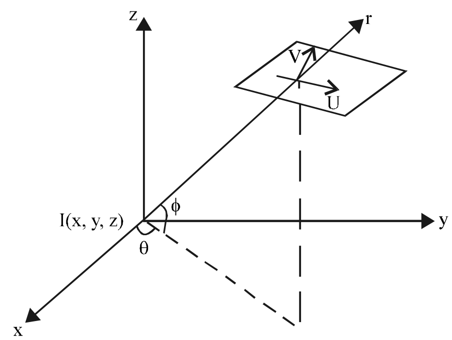

Fig. 3: Projected coordinate systems, I(x, y, z): The density of point (x, y, z), r: The projection direction

$$P_{\theta\phi}(u, v) = \int I(x, y, z) dr \quad (12)$$

This model is projected to produce the two dimensional projection data in four directions. The projection angle of the four directions are (0°, 0°), (0°, 45°), (0°, 90°), (0°, 135°).

Reconstruction results and analysis: In this review, three common reconstruction iterative algorithms of the CT image reconstruction field, i.e., the Algebraic Reconstruction Technique (ART), the Simultaneous Iterative Reconstruction algorithm (SIRT) and the Simultaneous Algebraic Reconstruction Technique (SART), are applied to the reconstruct the 3D image of the implosion-pellet in ICF experiment. These algorithms are used to detect the compression symmetry of the pellet in the experiment. In order to measure the quality of the reconstruction of different algorithms, the following three measures which are (Dominique and Michael, 2008), Normalized Mean Square Distance Measurement (NMSDM) value d, Normalized Absolute Distance

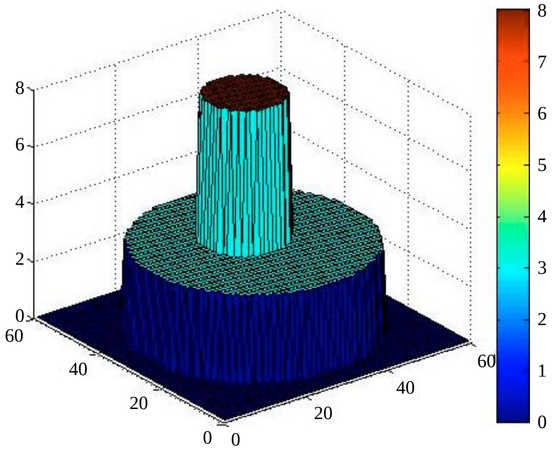

Fig. 4: Original image (Z = 0), Z = 0: The section of the model

Measurement (NADM) values r and Average Error (AE) e are adopted. A small number of big deviation between original pixels value and the reconstructed pixels will make d change a lot; r represents the importance of many small errors, which means that r is more sensitive to small errors of many elements; e means the total mismatch error between the original image and the reconstructed image. The smaller the value of these measures are, the better the reconstruction algorithm works. And these measures can also be used as iteration stopping conditions in the image reconstruction:

$$d = \left[\frac{\sum_{j=1}^{N} (x_j^* - x_j)^2}{\sum_{j=1}^{N} (x_j^* - \bar{x})^2} \right]^{1/2} \tag{13}$$

$$r = \frac{\sum_{j=1}^{N} \left| x_j^* - x_j \right|}{\sum_{j=1}^{N} \left| x_j \right|} \tag{14}$$

$$e = \sum_{j=1}^{N} \frac{\left| x_j^* - x_j \right|}{x_{max} \times N} \tag{15}$$

Z = 0 is selected as the reconstruction object and the spatial resolution of the reconstruction region is 60×60, the maximum sampling points is 170 in each projection direction, as shown in Fig. 4.

The reconstruction images under noise-free conditions are shown in Fig. 5a-c and the reconstruction images of the three algorithms are shown in Fig. 6a-c with the noise level of 15 dB.

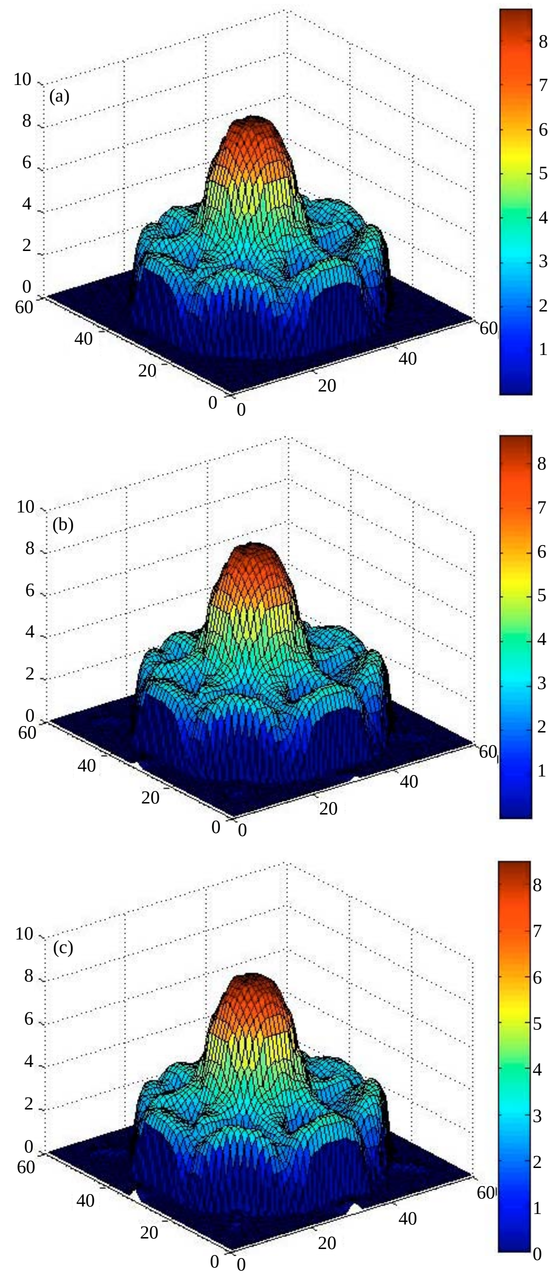

Fig. 5(a-c): Reconstruction image of (a) ART, (b) (SIRT) and (c) SART (SNR = +∞), ART: Algebraic reconstruction technique, SNR: Signal noise ratio, SIRT: Simultaneous iterative reconstruction technique, SART: Simultaneous algebraic reconstruction technique

Projection data are often inevitably affected by noise during the actual reconstruction process. Therefore, the

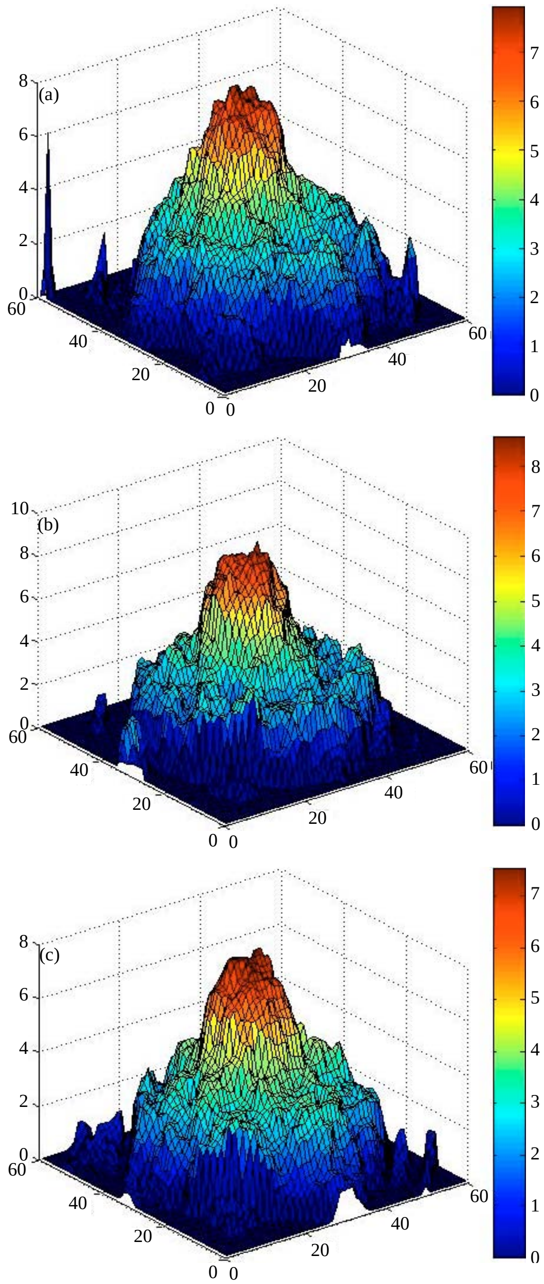

Fig. 6(a-c): Reconstruction image of (a) ART, (b) SIRT and (c) SART (SNR = 15), ART: Algebraic reconstruction technique, SNR: Signal noise ratio, SIRT: Simultaneous iterative reconstruction technique, SART: Simultaneous algebraic reconstruction technique

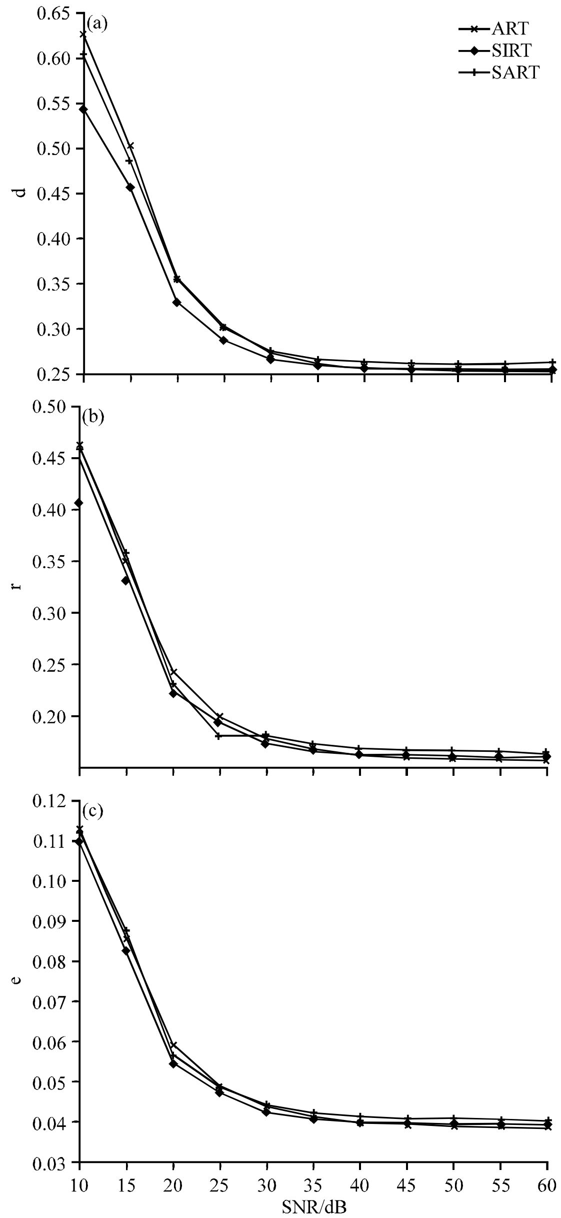

Fig. 7(a-c): (a) Normalized mean square distance measurement, (b) Normalized absolute distance measurement and (c) Average error

projection data is mixed with noise of different intensity and the reconstruction result of the three algorithms are shown in Fig. 7a-c. The optimal relaxation parameter of each algorithm when projection data contaminated with a specific level noise is tuned to achieve the best reconstruction result. The optimal relaxation parameter for each algorithm is shown in Fig. 8.

As shown in Fig. 5, with the noise-free projection data, all the three algorithms can reconstruct the original image fair well. Figure 7 shows that the ART algorithm is the best one and that the reconstruction accuracy of the

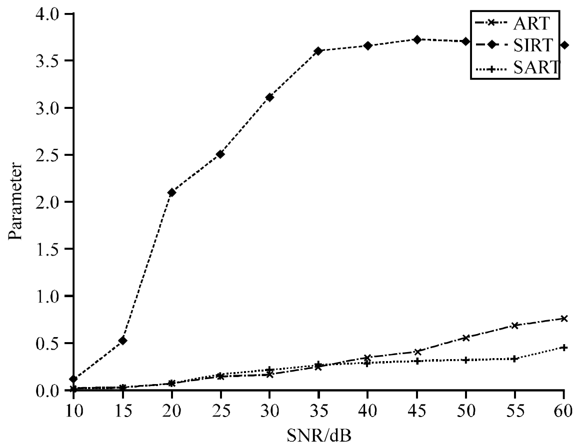

Fig. 8: Optimal relaxation parameter

three algorithms is comparable when the noise is weak (such as the SNR is 50 dB). That is, the ART algorithm performs best with the projection data contaminated by weak noise or without noise. In Fig. 8, as the noise intensity increases, the SIRT produces better results, even when the noise level is relatively high. As shown in Fig. 6, the reconstruction image of SIRT much similar to the original image than the other two algorithms when the SNR is 15. Furthermore, as is shown in Fig. 7, the reconstruction error of SIRT is smaller than the other two. Therefore, the SIRT is the best choice when the projection data is contaminated by high level noise.

CONCLUSION

Images captured by Framing cameras or pinhole cameras is a two-dimensional image without more detailed information. It can only reflect the contours of the pellet, which is difficult to make a precise diagnosis of the pellet compression symmetry. To overcome these shortcomings, three reconstruction algorithms are validated in the 3D image reconstruction of implosion pellet of ICF experiment. The numerical simulations results shows that the ART algorithm performs best in the 'incomplete' and noise-free projection data, in other words, the ART algorithm can reconstruct the 3D image with four two-dimensional projections. But the SIRT algorithm has better results when the projection data contaminated by high level noise. So, with the projection data is 'incomplete' and contaminated, the SIRT algorithm outperforms the other two algorithms.

ACKNOWLEDGMENT

This study is supported by the National High Technology Research and Development Program of China (863 Program) with No. 2011AA80XXXXX.

REFERENCES

Anders, H., 1989. Algebraic reconstruction in CT from limited views. Proceedings of the 8th IEEE Transaction on Medical Imaging, March, 1989, Sydney, Australia, pp: 50-55.

Andersen, A.H. and A.C. Kak, 1984. Simultaneous algebraic reconstruction technique (SART): A superior implementation of the ART algorithm. Ultrason Imaging, 2: 81-94.

Bin, Y., Z. Kai, Z. Pei-Ping, H. Wan-Xia and Y. Qing-Xi *et al*., 2008. The application of algebraic reconstruct technique in X-ray refraction contrast CT. Acta Phys. Sinica, 57: 3410-3418.

Buzmakov, A., D. Nikolaev, M. Chukalina and G. Schaefer, 2011. Efficient and effective regularized ART for computed tomography. Proceeding of the Annual International Conference of the IEEE Engineering in Medicine and Biology Society, August 30-September 3, 2011, Boston, MA., USA., pp: 6200-6203.

Dominique, V.S. and B. Michael, 2008. A systematic performance analysis of the simultaneous algebraic reconstruction technique (SART) for limited angle tomography. Proceedings of 30th Annual International IEEE EMBS Conference, August 20-24, 2008, British Columbia, Canada, pp: 20-24.

Guo, W. and H.X. Chen, 2009. Modified algebraic reconstruction algorithm and its implementation. J. Jilin Univ., 39: 39-41.

He, X.T., 2000. Progress and prospects of inertial confinement fusion research. Nuclear Sci. Eng., 20: 249-251.

Herman, G.T., 1980. Image Reconstruction from Projections: The Fundamentals of Computerized Tomography. Academic Press, New York.

Kaczmarz, S., 1937. Angenaherte auflosung von systemen linearer gleichungen. Bull. Int. Acad. Polon. Sci. Lett., 35: 355-357.

Liang-Zhong, X., X. Da, G. Huai-Min, Y. Di-Wu, Y. Si-Hua and Z. Lu-Ming, 2007. Photoacoustic imaging of blood vessels based on modified simultaneous iterative reconstruction technique. Acta Phys. Sin., 56: 3911-3916.

Liu, X., 2004. The study of the image reconstruction algorithm of industrial CT by computer simulation. J. Sichuan Univ., 32: 45-69.

Peng, S.X., F. Wang, D.R. Tang, S.Y. Liu and T.H. Huang *et al*., 2011. Inertial confinement fusion reaction rate measurement. Laser Particle Beams, 23: 2197-2220.

Yuan, Z., S.Y. Liu, Z. Cao, X. Sha-Li, H. Li, H. Zhang and L. Wang, 2009. Gain attenuation of gated framing camera. Laser and Particle Beams, 21: 704-708.

Zhang, J. and T.Q. Chang, 2004. Physical Fundament of Laser Nuclear Fusion Pellet. National Defense Industry Press, Beijing.

Zhang, R.F., 2008. Fast iterative algorithm for CT image reconstruction and analysis. J. Guilin Univ. Technol., 13: 34-38.

Zhang, S.L., 2005. Study and comparison of several reconstruction models of ART algorithm. Aeronautical Comput. Technol., 35: 39-41.

Zhang, S.L., D.H. Zhang and X.B. Zhao, 2007. ART algorithm study for industrial CT image reconstruction. Non-Destructive Testing, 29: 453-456.

Zhuang, T.G., 1992. CT Principles and Algorithms. Shanghai Jiaotong University Press, ShangHai.